

# Directed Flow of Baryons in Heavy-Ion Collisions

Yu.B. Ivanov<sup>a,b</sup>, E.G. Nikonov<sup>a,c</sup>, W. Nörenberg<sup>a</sup>,  
A.A. Shanenko<sup>c</sup>, and V.D. Toneev<sup>a,c</sup>

<sup>a</sup> *Gesellschaft für Schwerionenforschung mbH, Planckstr. 1, 64291 Darmstadt, Germany*

<sup>b</sup> *Kurchatov Institute, Kurchatov sq. 1, Moscow 123182, Russia*

<sup>c</sup> *Joint Institute for Nuclear Research, 141980 Dubna, Moscow Region, Russia*

The collective motion of nucleons from high-energy heavy-ion collisions is analyzed within a relativistic two-fluid model for different equations of state (EoS). As function of beam energy the theoretical slope parameter  $F_y$  of the differential directed flow is in good agreement with experimental data, when calculated for the QCD-consistent EoS described by the statistical mixed-phase model. Within this model, which takes the deconfinement phase transition into account, the excitation function of the directed flow  $\langle P_x \rangle$  turns out to be a smooth function in the whole range from SIS till SPS energies. This function is close to that for pure hadronic EoS and exhibits no minimum predicted earlier for a two-phase bag-model EoS. Attention is also called to a possible formation of nucleon antiflow ( $F_y < 0$ ) at energies  $\gtrsim 100$  A·GeV.

PACS numbers: 24.85.+p, 12.38.Aw, 12.38Mh, 21.65.+f, 64.60.-i, 27.75.+r

## I. INTRODUCTION

Collective flows of various types (radial, directed, elliptic,...) observed experimentally in heavy-ion collisions reveal a space-momentum correlated motion of strongly interacting nuclear matter. This collective motion is essentially caused by the pressure gradients arising during the time evolution in the collision, and hence opens a promising way for obtaining information on the equation of state (EoS) and, in particular, on a possible phase transition. Recently, this feature has stimulated a large number of experimental and theoretical investigations on flow effects (cf. review articles [1,2]).

Manifestations of the deconfinement phase transition have been considered already some time ago by Shuryak, Zhurov [3] and van Hove [4]. Since a phase transition slows down the time evolution of the system due to *softening* of the EoS, the authors expect around some critical incident energy a remarkable loss of correlation between the observed particle momenta and the reaction plane, and hence a reduction of the directed flow. Assuming a first-order phase transition Hung, Shuryak [5] and Rischke et al. [6] have recently obtained quantitative predictions for heavy-ion collisions. For an expanding fireball Hung and Shuryak expect the *softest point* effect around  $E_{lab} = 30$  A·GeV. Within a one-fluid hydrodynamic model Rischke et al. show that the excitation function of the directed flow exhibits a deep minimum near  $E_{lab} = 6$  A·GeV. However, preliminary experimental results [7] in this energy range do not confirm these predictions. In the following, we report on a study of the directed flow within a two-fluid hydrodynamic model [8] for the statistical mixed-phase EoS [9,10] which is adjusted to available lattice QCD data.

## II. EQUATION OF STATE WITHIN THE MIXED-PHASE MODEL

Our consideration is essentially based on the recently proposed Mixed-Phase (MP) model [9,10] which is consistent with available QCD lattice data [11]. The underlying assumption of the MP model is that unbound quarks and gluons *may coexist* with hadrons forming a *homogeneous* quark/gluon-hadron phase. Since the mean distance between hadrons and quarks/gluons in this mixed phase may be of the same order as that between hadrons, the interaction between all these constituents (unbound quarks/gluons and hadrons) plays an important role and defines the order of the phase transition.

Within the MP model [9,10] the effective Hamiltonian is expressed in the quasiparticle approximation with density-dependent mean-field interactions. Under quite general requirements of confinement for color charges, the mean-field potential of quarks and gluons is approximated by

$$U_q(\rho) = U_g(\rho) = \frac{A}{\rho^\gamma}; \quad \gamma > 0 \quad (1)$$

with the total density of quarks and gluons

$$\rho = \rho_q + \rho_g + \sum_j \nu_j \rho_j,$$

where  $\rho_q$  and  $\rho_g$  are the densities of unbound quarks and gluons outside of hadrons, while  $\rho_j$  is the density of hadron type  $j$  and  $\nu_j$  is the number of valence quarks inside. The presence of the total density  $\rho$  in (1) implies interactions between all components of the mixed phase. The approximation (1) mirrors two important limits of the QCD interaction. For  $\rho \rightarrow 0$ , the interaction potential approaches infinity, *i.e.* an infinite energy is necessary to create an isolated quark or gluon, which simulates

the confinement of color objects. In the other extreme case of large energy density corresponding to  $\rho \rightarrow \infty$ , we have  $U_q = U_g = 0$  which is consistent with asymptotic freedom.

The use of the density-dependent potential (1) for quarks and the hadronic potential, described by a modified non-linear mean-field model [12], requires certain constraints to be fulfilled, which are related to thermodynamic consistency [9,10]. For the chosen form of the Hamiltonian these conditions require that  $U_g(\rho)$  and  $U_q(\rho)$  do not depend on temperature. From these conditions one also obtains a form for the quark-hadron potential [9].

A detailed study of the pure gluonic  $SU(3)$  case with a first-order phase transition allows one to fix the values of the parameters as  $\gamma = 0.62$  and  $A^{1/(3\gamma+1)} = 250$  MeV. These values are then used for the  $SU(3)$  system including quarks. As is shown in Fig.1 for the case of quarks of two light flavors at zero baryon density ( $n_B = 0$ ), the MP model is consistent with lattice QCD data providing a continuous phase transition of the cross-over type with a deconfinement temperature  $T_{dec} = 153$  MeV. For a two-phase approach based on the bag model a first-order deconfinement phase transition occurs with a sharp jump in energy density  $\varepsilon$  at  $T_{dec}$  close to the value obtained from lattice QCD.

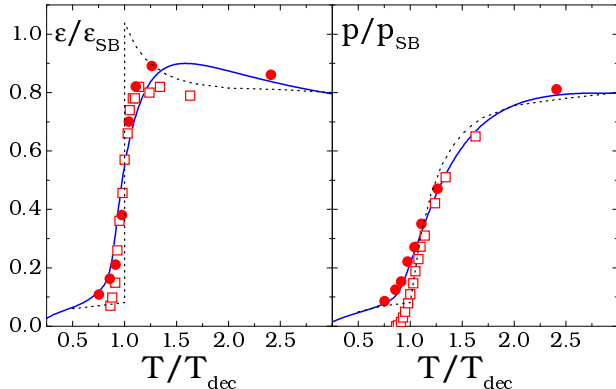


FIG. 1. The reduced energy density  $\varepsilon/\varepsilon_{SB}$  and pressure  $p/p_{SB}$  (the  $\varepsilon_{SB}$  and  $p_{SB}$  are corresponding Stephan-Boltzmann quantities) of the  $SU(3)$  system with two light flavors for  $n_B = 0$  calculated within the MP (solid lines) and bag (dashed lines) models. Circles and squares are lattice QCD data obtained within the Wilson [13] and Kogut-Susskind [14] schemes, respectively.

Though at a glimpse the temperature dependences of the energy density  $\varepsilon$  and pressure  $p$  for the different approaches presented in Fig.1 look quite similar, there are large differences revealed when  $p/\varepsilon$  is plotted versus  $\varepsilon$  (cf. Fig.2, left panel). The lattice QCD data differ at low  $\varepsilon$ , which is due to difficulties within the Kogut-Susskind scheme [14] in treating the hadronic sector. A particular feature in the MP model is that, for  $n_B = 0$ , the *softest point* of the EoS, defined as a minimum of the function

$p(\varepsilon)/\varepsilon$  [5], is not very pronounced and located at comparatively low values of the energy density:  $\varepsilon_{SP} \approx 0.45$  GeV/fm<sup>3</sup>, which roughly agrees with the lattice QCD value [13]. This value of  $\varepsilon$  is close to the energy density inside the nucleon, and hence, reaching this value indicates that we are dealing with a single *big hadron* consisting of deconfined matter. In contradistinction, the bag-model EoS exhibits a very pronounced softest point at large energy density  $\varepsilon_{SP} \approx 1.5$  GeV/fm<sup>3</sup> [5,6].

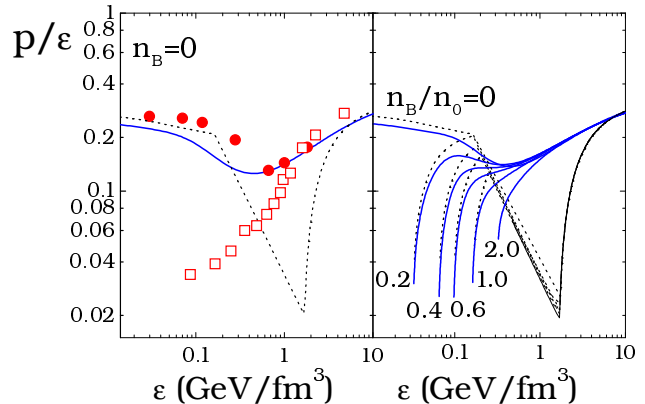


FIG. 2. The  $(\varepsilon, p/\varepsilon)$ -representation of the EoS for the two-flavor  $SU(3)$  system at various baryon densities  $n_B$ . Notation of data points and lines is the same as in Fig.1.

The MP model can be extended to baryon-rich systems in a parameter-free way [9,10]. As demonstrated in Fig.2 (right panel), the softest point for baryonic matter is gradually washed out with increasing baryon density and vanishes for  $n_B \gtrsim 0.4 n_0$  ( $n_0$  is normal nuclear matter density). This behavior differs drastically from that of the two-phase bag-model EoS, where  $\varepsilon_{SP}$  is only weakly dependent on  $n_B$  [5,6]. It is of interest to note that the interacting hadron gas model has no softest point at all and, in this respect, its thermodynamic behavior is close to that of the MP model at high energy densities [10].

These differences between the various models should manifest themselves in the dynamics discussed below.

### III. TWO-FLUID HYDRODYNAMIC MODEL

In contrast to the one-fluid hydrodynamic model, where local instantaneous stopping of projectile and target matter is assumed, a specific feature of the dynamical two-fluid description is a finite stopping power. Experimental rapidity distributions in nucleus-nucleus collisions support this specific feature of the two-fluid model. In accordance with [8], the total baryonic current and energy-momentum tensor are written as

$$J^\mu = J_p^\mu + J_t^\mu, \quad (2)$$

$$T^{\mu\nu} = T_p^{\mu\nu} + T_t^{\mu\nu}, \quad (3)$$

where the baryonic current  $J_\alpha^\mu = n_\alpha u_\alpha^\mu$  and energy-momentum tensor  $T_\alpha^{\mu\nu}$  of the fluid  $\alpha$  are initially associated with either target ( $\alpha = t$ ) or projectile ( $\alpha = p$ ) nucleons. Later on – while heated up – these fluids contain all hadronic and quark–gluon species, depending on the model used for describing the fluids. The twelve independent quantities (the baryon densities  $n_\alpha$ , 4-velocities  $u_\alpha^\mu$  normalized as  $u_{\alpha\mu}u_\alpha^\mu = 1$ , as well as temperatures and pressures of the fluids) are obtained by solving the following set of equations of two-fluid hydrodynamics [8]

$$\partial_\mu J_\alpha^\mu = 0 \quad , \quad (4)$$

$$\partial_\mu T_\alpha^{\mu\nu} = F_\alpha^\nu \quad , \quad (5)$$

where the coupling term

$$F_\alpha^\nu = n_p^s n_t^s \left\langle V_{rel} \int d\sigma_{NN \rightarrow NX}(s) (p - p_\alpha)^\nu \right\rangle \quad (6)$$

characterizes friction between the counter-streaming fluids. Here,  $n_\alpha^s$  and  $(p - p_\alpha)$  denote respectively the scalar density of the fluid and the 4-momentum transfer gained by a particle of the fluid  $\alpha$  after collision with a particle of the counter-streaming fluid. The cross sections  $d\sigma_{NN \rightarrow NX}$  take into account all elastic and inelastic interactions between the constituents of different fluids at the invariant collision energy  $s^{1/2}$  with the local relative velocity  $V_{rel} = [s(s - 4m_N^2)]^{1/2}/2m_N^2$ . The average in (6) is taken over all particles in the two fluids which are assumed to be in local equilibrium intrinsically [8]. The set of Eqs. (4) and (5) is closed by an EoS, which is naturally the same for both colliding fluids.

The friction term  $F_\alpha^\nu$  in Eq. (5) originates from both elastic and inelastic  $NN$  collisions. The latter give rise to a direct emission of mesons in addition to the thermal mesons in the fluids. In the present version only for the pions the direct emission is included by the additional equations

$$\partial_\nu J_\pi^\nu = n_p^s n_t^s \left\langle V_{rel} \int d\sigma_{NN \rightarrow \pi X} \right\rangle \quad , \quad (7)$$

$$\partial_\mu T_\pi^{\mu\nu} = n_p^s n_t^s \left\langle V_{rel} \int d\sigma_{NN \rightarrow \pi X} p_\pi^\nu \right\rangle \quad , \quad (8)$$

where  $p_\pi$  is the 4-momentum of an emitted direct pion. These equations together with (5) provide the total energy–momentum conservation

$$\partial_\mu (T_\pi^{\mu\nu} + T_p^{\mu\nu} + T_t^{\mu\nu}) = 0 \quad . \quad (9)$$

It is assumed [8] that in the subsequent evolution these direct pions interact neither with the fluids nor with each other. This is a reasonable assumption at relativistic energies, simulating a long formation time of these direct pions. At moderate energies, where the latter argument does not hold in general, the number of direct pions is negligible compared to the number of thermal pions.

For the calculation of the friction force (6), approximations of  $N$ - $N$  cross-sections are used. It was found [15]

that a part of the friction term, which is related to the transport cross-section, may be well parametrized by an effective deceleration length  $\lambda_{\text{eff}}$  with a constant value  $\lambda_{\text{eff}} \approx 5$  fm. However, there are reasons to consider  $\lambda_{\text{eff}}$  as a phenomenological parameter, as it was pointed out in [8]. First, the value of  $\lambda_{\text{eff}}$  is highly sensitive to the precise form of parameterization of the free cross-sections which, in addition, may be essentially modified by in-medium effects. Furthermore, the model neglects the interactions of direct pions both with each other and with baryons, as well as the direct emission of other mesons which are produced quite abundantly at SPS energies. Due to all these effects the stopping power at SPS energies is somewhat underestimated [8]. This shortcoming of the model is cured by an appropriate choice of the  $\lambda_{\text{eff}}$  value as

$$\lambda_{\text{eff}} = a \exp(-b\sqrt{s})$$

with  $a = 6.6$  fm and  $b = 0.106$  GeV $^{-1}$  adjusted to the rapidity distributions of nucleons and pions in central Au+Au collisions at AGS and SPS energies.

Following the original paper [8], it is assumed that a fluid element decouples from the hydrodynamic regime, when its baryon density  $n_B$  and densities in the eight surrounding cells become smaller than a fixed value  $n_f$ . A value  $n_f = 0.8n_0$  was used for this local freeze-out density which corresponds to the actual density of the frozen-out fluid element of about  $0.5n_0$  to  $0.7n_0$ .

#### IV. COLLECTIVE FLOW FROM HEAVY-ION COLLISIONS

For central nucleus–nucleus collisions only the isotropic transverse expansion, or transverse radial flow, develops due to the azimuthal symmetry of a system. The presence of the reaction plane for non-central collisions destroys this symmetry and gives rise to various patterns of collective motion generated by compressed and excited nuclear matter created during the collision. For example, the directed (or sideward) flow characterizes the deflection of emitted hadrons away from the beam axis within the reaction plane. In particular, one defines the differential directed flow by the mean in-plane component  $\langle p_x(y) \rangle$  of the transverse momentum at a given rapidity  $y$ . This deflection is believed to be quite sensitive to the *elasticity* or *softness* of the EoS.

The  $\langle p_x(y) \rangle$  distributions of baryons are shown in Fig.3 for Au+Au collisions at  $E_{lab} = 10$  A·GeV calculated for different EoS at an impact parameter  $b = 3$  fm. In general, the characteristic  $S$ -shape of the distribution is reproduced, demonstrating a definite anti-correlation between nucleons bounced-off from the target and projectile regions. One should keep in mind that the protons bound in observed complex particles (*e.g.*, in deuterons) are not excluded in our calculations. Therefore, all hydrodynamic results should be compared to the triangle

points in Fig.3, where nucleons from complex particles do contribute. The MP and interacting hadronic models\* give similar results, both getting into error bars of these triangle points, though the flow in the MP model is slightly lower due to softening of EoS near the crossover phase transition. This softening is stronger for the bag-model EoS. However, one should note that different versions of

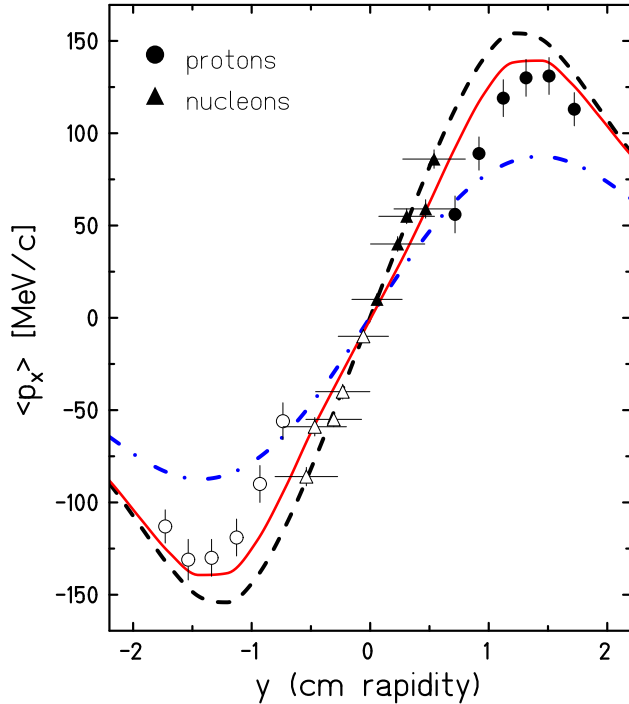


FIG. 3. Differential directed flow of nucleons in the reaction plane as a function of rapidity in semi-central (the trigger transverse energy  $E_T = (200 - 230)$  GeV) Au + Au collisions at the energy 10 A-GeV. Three curves are calculated within relativistic two-fluid hydrodynamics for an impact parameter  $b = 3$  fm and different EoS: for the MP model (solid line), interacting hadron gas model (dashed) and two-phase bag model (dot-dashed). Circles are experimental points for identified protons, triangles correspond to a nucleon flow estimate based on the measurement of  $E_T$  and the number of charged particles  $N_C$  [16]. Experimental points marked by full symbols are measured directly, open ones are obtained by reflecting at the mid-rapidity point.

transport codes, which do not account for a phase transition, also give a reasonable description of  $\langle p_x(y) \rangle$  (e.g., see the comparison with RQMD results in [16]). Therefore, convincing evidence on a possible phase transition,

\*The interaction in the hadron model is taken into account in the same manner as that in the hadronic sector of the MP model [9,10].

based solely on the data at a single bombarding energy, is hardly possible.

The rapidity dependence of the mean in-plane transverse momentum can be quantified in terms of the derivative at mid-rapidity

$$F_y = \left. \frac{d \langle p_x(y) \rangle}{dy} \right|_{y=y_{cm}}, \quad (10)$$

which is quite suitable for analyzing the flow excitation function. The slope parameter  $F_y$  calculated with the MP-model EoS is presented in Fig.4 (upper panel) together with available experimental points covering the whole range of incident energies. The results describe correctly the decrease of  $F_y$  with increasing energy and shows essentially no dependence on impact parameter for semi-central collisions. It was shown experimentally [17] that the directed flow is larger for heavier fragments. As mentioned before, hydrodynamic calculations deal with *primordial* nucleons, and hence they describe the mean value of  $F_y$  for free nucleons and nucleons bound in deuterons and heavier fragments. Therefore, our hydrodynamic results lie between the experimental points for identified protons (open circles in Fig.4) and the data [17] (full circles in Fig.4) for intermediate mass fragments<sup>†</sup>. This effect is particularly strong for energies below  $E_{lab} \approx 1$  A-GeV, where the baryonic flow is largest (and heavy fragments in the mid-rapidity range are abundant).

To our knowledge no other hydrodynamic calculations of  $F_y(E_{lab})$  have been reported. Therefore, we compare our results with transport calculations in the lower panel of Fig.4. The ARC and ART are cascade models, while the RQMD takes also into account mean-field effects. Though all these models agree with experimental data at  $E_{lab} \approx 10$  A-GeV (considered as a reference point), values of  $F_y$  at lower energies are clearly underestimated, as is evident from comparison with preliminary results of the E895 Collaboration [7] (see empty squares in Fig.4). Recently, a good description of experimental points (including the E895 data) was reported within a relativistic BUU (RBUU) model [21]. The good agreement with experiment was achieved by a special fine tuning of the mean fields involved in the particle propagation.

<sup>†</sup>For complex particles the value  $F_y$  was deduced from  $p_x$  per baryon. The FOPI data for intermediate mass fragments are often scaled by factor 0.7 to make absolute values comparable to those for  $p, d, \alpha$  [17]. We do not use this scaling factor. Note that everywhere we deal with  $F_y$  defined by Eq.(10), which differs from the frequently used flow parameter  $F = F_y y_{cm}$ . The extra beam-rapidity factor  $y_{cm}$  obscures a relative role of dynamical effects in the energy dependence of the directed-flow slope parameter.

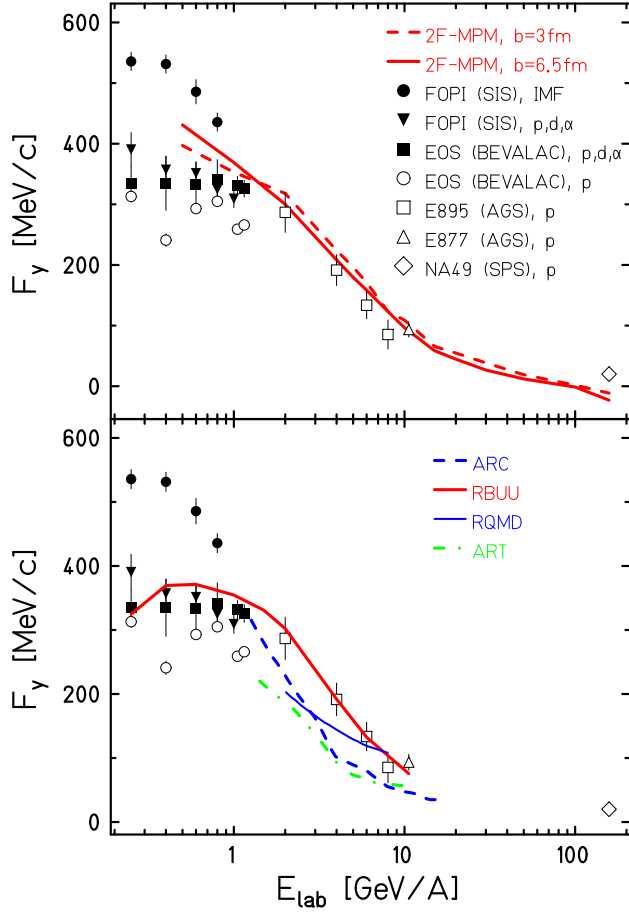


FIG. 4. Excitation function of the slope parameter  $F_y$  for baryons from Au + Au collisions within two-fluid hydrodynamics for the MP EoS (upper panel) and within different transport simulations (lower panel). Open symbols are experimental points for identified protons (see data collection in [2,17,18]), filled circles, triangles and squares correspond to the flow parameter measured for intermediate mass fragments [17] and for light particles  $p, d, \alpha$  [19,20]. The results of transport calculations for three different codes are given by the thin solid (RQMD), dashed (ARC) and dot-dashed (ART) lines (cited according to [18]). The solid line (RBUU) is taken from [21].

It is of interest to mention that the calculated value of  $F_y$  for the baryon flow becomes negative (antiflow) for beam energies  $\gtrsim 100$  A·GeV, while the experiment [22] gives a small but positive value even at 158 A·GeV. The reason of this antiflow is a wiggle in the  $\langle p_x(y) \rangle$  distribution arising in hydrodynamic results within a narrow mid-rapidity interval  $|\delta y| \lesssim 1$  due to a peculiar interplay between the transverse radial and directed flows. The possibility of such an effect was noticed in [23] some time ago and later also observed in the UrQMD transport calculations [24]. However, actual measurements have been taken at larger rapidities and then extrapolated into this unmeasured region [22]. Therefore, more accurate data in the mid-rapidity region are necessary to clarify this

behavior.

The directed flow can be characterized by another quantity which is less sensitive to possible rapidity fluctuations of the in-plane momentum. Such a quantity is the average directed flow which is defined by

$$\langle P_x \rangle = \frac{\int dp_x dp_y dy p_x \left( E \frac{d^3 N}{dp^3} \right)}{\int dp_x dp_y dy \left( E \frac{d^3 N}{dp^3} \right)}, \quad (11)$$

where the integration in the c.m.system runs over the rapidity region  $[0, y_{cm}]$ . The calculated excitation functions for the average directed flow of baryons within different models are shown in Fig.5. Conventional (one-fluid) hydrodynamics for pure hadronic matter [6] results

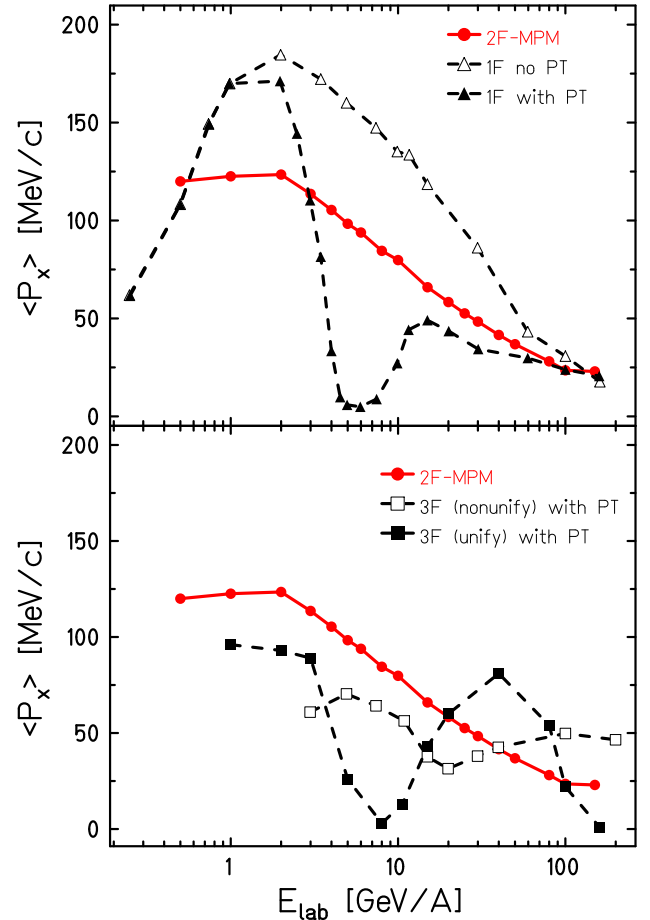


FIG. 5. The excitation function of the average directed flow for baryons from Au + Au collisions. Two-fluid hydrodynamics with the MP EoS at the impact parameter 3 fm is compared with the corresponding results of one-fluid [6] (upper panel) and three-fluid (lower panel) [25] hydrodynamics with the bag-model EoS. One-fluid calculations both with and without the phase transition (PT) are displayed.

in a very large directed flow due to the inherent instantaneous stopping of the colliding matter. This instant-

neous stopping is unrealistic at high beam energies. If the deconfinement phase transition, based on the bag-model EoS [6], is included into this model, the excitation function of  $\langle P_x \rangle$  exhibits a deep minimum near  $E_{lab} \approx 6$  A·GeV, which manifests the softest-point effect of the bag-model EoS depicted in the right panel of Fig.2.

The result of two-fluid hydrodynamics with the MP EoS noticeably differs from the one-fluid calculations. After a maximum around 1 A·GeV, the average directed flow decreases slowly and smoothly. This difference is caused by two reasons. First, as follows from Fig.2, the softest point of the MP EoS is washed out for  $n_B \gtrsim 0.4$ . The second reason is dynamical: the finite stopping power and direct pion emission change the evolution pattern. The latter point is confirmed by comparison to three-fluid calculations with the bag EoS [25] plotted in the lower panel of Fig.5. The third pionic fluid in this model is assumed to interact only with itself neglecting the interaction with baryonic fluids. Therefore, with regard to the baryonic component, this three-fluid hydrodynamics [25,26] is completely equivalent to our two-fluid model and the main difference is due to the different EoS. As seen in Fig.5, the minimum of the directed flow excitation function, predicted by the one-fluid hydrodynamics with the bag EoS, survives in the three-fluid (nonunified) regime but its value decreases and its position shifts to higher energies. If one applies the *unification procedure* of [25], which favors fusion of two fluids into a single one, and thus making stopping larger, three-fluid hydrodynamics practically reproduces the one-fluid result and predicts in addition a bump at  $E_{lab} \approx 40$  A·GeV.

## V. CONCLUSIONS

We have studied relativistic nuclear collisions within 3D two-fluid hydrodynamics combined with different EoS, including that of the statistical mixed-phase model of the deconfinement phase transition, developed in [9,10]. It has been shown that the directed flow excitation functions  $F_y$  and  $\langle P_x \rangle$  for baryons are sensitive to the EoS, but this sensitivity is significantly masked by nonequilibrium dynamics of nuclear collisions. Nevertheless, the results indicate that the widely used two-phase EoS, based on the bag model [5,6] and giving rise to a first-order phase transition, seems to be inappropriate. The neglect of interactions near the deconfinement temperature results in an unrealistically strong softest-point effect within this two-phase EoS. In fact, its prediction of a minimum in  $\langle P_x \rangle(E_{lab})$  near  $E_{lab} \approx 6$  A·GeV has not been confirmed experimentally [7]. However, accurate experimental investigations of the differential directed flow and flow excitation functions in the energy region between AGS and SPS are still highly demanded not only in searching for a shifted minimum of  $\langle P_x \rangle(E_{lab})$ , but also in clarifying the physics of a possible negative slope (antiflow) of the baryonic directed flow  $F_y$ . This antiflow

is particularly sensitive to the EoS. While for the EoS in the MP model the antiflow is predicted at incident energies only above 100 A·GeV, it occurs already at 8 A·GeV, when the bag EoS is used [25].

In this respect a dramatic phenomenon of the *cracked nut* proposed recently as a hydrodynamic signature of the QCD phase transition at RHIC and LHC energies [27,28] looks questionable. The authors argue that the softest point in the EoS may lead to the development of two shells at the edge of the almond-like initial fireball, which are then cracked by internal pressure and separated, resulting in a specific flow pattern. However, this speculation was based on the bag-model EoS. The application of the QCD-consistent EoS of the MP model to this problem would be interesting.

The directed flow is the first coefficient in the Fourier decomposition of the azimuthal momentum distribution of particles [29]. The second coefficient, the elliptic flow, is expected to be more sensitive to the EoS and some hints of the phase transition have been indicated by an analysis of the measured excitation function for the elliptic flow (see review articles [1,2]). The study of the elliptic flow within two-fluid hydrodynamics for the mixed-phase model EoS is in progress.

## ACKNOWLEDGMENTS

We are grateful to V. Russkikh for making his hydrodynamic code available to us. We thank P. Danielewicz, B. Friman and E. Kolomeitsev for useful discussions. Yu.B.I., E.G.N. and V.D.T. gratefully acknowledge the hospitality at the Theory Group of GSI, where this work has been done. This work was supported in part by DFG (project 436 RUS 113/558/0) and RFBR (grant 00-02-04012). Yu.B.I. was partially supported by RFBR grant 00-15-96590.

- 
- [1] P. Braun-Munzinger and J. Stachel, Nucl. Phys. **A638**, 3c (1998).
  - [2] P. Danielewicz, Nucl. Phys. **A661**, 82c (1999).
  - [3] E. Shuryak and O.V. Zhironov, Phys. Lett. B **89**, 253 (1979).
  - [4] L. van Hove, Z. Phys. C **21**, 93 (1983).
  - [5] C.M. Hung and E.V. Shuryak, Phys. Rev. Lett. **75**, 4003 (1995); Phys. Rev C **57**, 1891 (1998).
  - [6] D.H. Rischke, Y. Pürsün, J.A. Maruhn, H. Stöcker, and W. Greiner, Heavy Ion Phys. **1**, 309 (1996); D.H. Rischke, Nucl. Phys. **A610**, 88c (1996).
  - [7] H. Liu for the E895 Collaboration, Nucl. Phys. **A638**, 451c (1998).
  - [8] I.N. Mishustin, V.N. Russkikh, and L.M. Satarov, Nucl.

- Phys. **A494**, 595 (1989); *Yad. Fiz.* **54**, 429 (1991) (translated as *Sov. J. Nucl. Phys.* **54**, 260 (1991)).
- [9] E.G. Nikonov, A.A. Shanenko, and V.D. Toneev, *Heavy Ion Phys.* **8**, 89 (1998); nucl-th/9802018.
- [10] V.D. Toneev, E.G. Nikonov, and A.A. Shanenko, in *Nuclear Matter in Different Phases and Transitions*, eds. J.-P. Blaizot, X. Campi, and M. Ploszajczak, Kluwer Academic Publishers (1999), pp.309-320; Preprint GSI 98-30, Darmstadt, 1998.
- [11] See e.g. F. Karsch, Talk given at the *Strong and Electroweak Matter '98*, December 1998, Copenhagen, hep-lat/9903031.
- [12] J. Zimanyi *et al.*, *Nucl. Phys.* **A484**, 647 (1988).
- [13] K. Redlich and H. Satz, *Phys. Rev. D* **33**, 3747 (1986).
- [14] C. Bernard *et al.*, *Nucl. Phys. (Proc. Suppl.)* **B47**, 499 (1996); *ibid* 503.
- [15] L.M. Satarov, *Sov. J. Nucl. Phys.* **52**, 264 (1990).
- [16] J. Barrette *et al.*, *Phys. Rev. C* **56**, 3254 (1997).
- [17] W. Reisdorf and H.G. Ritter, *Ann. Rev. Nucl. Part. Sci.* **47**, 663 (1997).
- [18] N.N. Ajitanand *et al.*, *Nucl. Phys.* **A638**, 451c (1998).
- [19] N. Herrmann, FOPI Collaboration, *Nucl. Phys.* **A610**, 49c (1996).
- [20] J. Chance *et al.* (The EOS Collaboration), *Phys. Rev. Lett.* **78**, 2535 (1997).
- [21] P.K. Sahu, W. Cassing, U. Mosel, and A. Ohnishi, *Nucl. Phys.* **A672**, 376 (2000).
- [22] H. Appelshäuser *et al.* (NA49 Collaboration), *Phys. Rev. Lett.* **80**, 4136 (1998).
- [23] S.A. Voloshin, *Phys. Rev. C* **55**, 1632 (1997).
- [24] S. Soff, S.A. Bass, M. Bleicher, H. Stöcker, and W. Greiner, nucl-th/9903061.
- [25] J. Brachmann *et al.*, *Phys. Rev. C* **61**, 024909 (2000).
- [26] J. Brachmann *et al.*, *Nucl. Phys.* **A619**, 391 (1997).
- [27] E.V. Shuryak, *Phys. Rev. D* **60**, 115014 (1999); D. Teaney and E.V. Shuryak, *Phys. Rev. Lett.* **83**, 4951 (1999).
- [28] P.F. Kolb, J. Sollfrank, and U. Heinz, *Phys. Lett.* **B459**, 667 (1999).
- [29] A.M. Poskanzer and S.A. Voloshin, *Phys. Rev. C* **58**, 1671 (1998).